nature COMMUNICATIONS

ARTICLE

Received 22 May 2014 | Accepted 1 Jul 2014 | Published 30 Jul 2014

DOI: 10.1038/ncomms5566

Direct observation of the spin texture in SmB_6 as evidence of the topological Kondo insulator

N. Xu[1], P.K. Biswas[2], J.H. Dil[1,3], R.S. Dhaka[1,3], G. Landolt[1,4], S. Muff[1,3], C.E. Matt[1,5], X. Shi[1,6], N.C. Plumb[1], M. Radović[1,7], E. Pomjakushina[8], K. Conder[8], A. Amato[2], S.V. Borisenko[9], R. Yu[6], H.-M. Weng[6,10], Z. Fang[6,10], X. Dai[6,10], J. Mesot[1,3,5], H. Ding[6,10] & M. Shi[1]

Topological Kondo insulators have been proposed as a new class of topological insulators in which non-trivial surface states reside in the bulk Kondo band gap at low temperature due to strong spin–orbit coupling. In contrast to other three-dimensional topological insulators, a topological Kondo insulator is truly bulk insulating. Furthermore, strong electron correlations are present in the system, which may interact with the novel topological phase. By applying spin- and angle-resolved photoemission spectroscopy, here we show that the surface states of SmB_6 are spin polarized. The spin is locked to the crystal momentum, fulfilling time reversal and crystal symmetries. Our results provide strong evidence that SmB_6 can host topological surface states in a bulk insulating gap stemming from the Kondo effect, which can serve as an ideal platform for investigating of the interplay between novel topological quantum states with emergent effects and competing orders induced by strongly correlated electrons.

[1] Swiss Light Source, Paul Scherrer Institut, CH-5232 Villigen, Switzerland. [2] Laboratory for Muon Spin Spectroscopy, Paul Scherrer Institut, CH-5232 Villigen, Switzerland. [3] Institute of Condensed Matter Physics, École Polytechnique Fédérale de Lausanne, CH-1015 Lausanne, Switzerland. [4] Physik-Institut, Universität Zürich, Winterthurerstrauss 190, CH-8057 Zürich, Switzerland. [5] Laboratory for Solid State Physics, ETH Zürich, CH-8093, Zürich, Switzerland. [6] Beijing National Laboratory for Condensed Matter Physics and Institute of Physics, Chinese Academy of Sciences, Beijing 100190, China. [7] SwissFEL, Paul Scherrer Institut, CH-5232 Villigen, Switzerland. [8] Laboratory for Developments and Methods, Paul Scherrer Institut, CH-5232 Villigen, Switzerland. [9] Institute for Solid State Research, IFW Dresden, PO Box 270116, D-01171 Dresden, Germany. [10] Collaborative Innovation Center of Quantum Matter, Beijing 100084, China. Correspondence and requests for materials should be addressed to N.X. (email: nan.xu@psi.ch) or to M.S. (email: ming.shi@psi.ch).

Despite the great success in understanding the physical properties of topological insulators (TIs), a crucial experimental and technological problem remains unresolved—namely, most three-dimensional (3D) TI candidates are not bulk insulating[1]. The bulk conducting band, as illustrated in Fig. 1b, makes it complicated to extract the topological surface properties from transport measurements and other bulk-sensitive measurements. Furthermore, the bulk conductivity prohibits TIs from being applied as spintronic materials and from realizing exotic novel phenomena, such as Majorana fermions. Aside from this issue, at present TIs are essentially understood within non-interacting topological theory[2,3] (Fig. 1b), and thus the consequences of strong electron correlations interacting with topological phases are still unknown.

Recent theoretical investigations[4–6] have suggested that some Kondo insulators such as SmB_6, in which electrons are strongly correlated, can possibly host non-trivial topological surface states (TSS) atop truly insulating bulk crystals, forming a special group of TIs known as topological Kondo insulators (TKIs). Our previous high-resolution angle-resolved photoemission spectroscopy (ARPES) study[7] has revealed that two-dimensional surface states reside within the Kondo band gap ($\Delta \sim 20$ meV relative to chemical potential) and form three Fermi surfaces (FSs) in the first surface Brillouin zone (SBZ): one is centred at the SBZ ($\bar{\Gamma}$ point in Fig. 1a) and two (viewed as four half-FSs) encircle the midpoints of the SBZ boundaries ($\bar{X}$ points) (Fig. 1c). The odd number of surface bands crossing the Fermi level (E_F) fulfills a necessary condition of TSS, and the observed surface state dispersions are in good agreement with theoretical calculations indicating that SmB_6 could be a TKI. Our observations are also consistent with transport results[8–15] and supported by other ARPES[16–18] studies, as well as scanning tunnelling microscopy measurements[19]. On the other hand, the in-gap states have also been discussed as topologically trivial polar surface states[20], and even as bulk states[21]. Until now, there has been no conclusive evidence indicating that SmB_6 is a TKI. Therefore, identifying the topologically non-trivial nature of the in-gap states of SmB_6 is crucial for distinguishing these different explanations and verifying whether SmB_6 is indeed the first realization of a TKI.

Using spin-resolved ARPES (SARPES), here we investigate the spin texture of the surface states around the $\bar{X}$ points in the SBZ of SmB_6. We show that the surface states are spin polarized with strong $\mathbf{k}_{||}$ dependence. The spin-helical structure fulfills the requirement of time-reversal symmetry (TRS). Our results give direct evidence that SmB_6 is the first realization of a strongly correlated TKI.

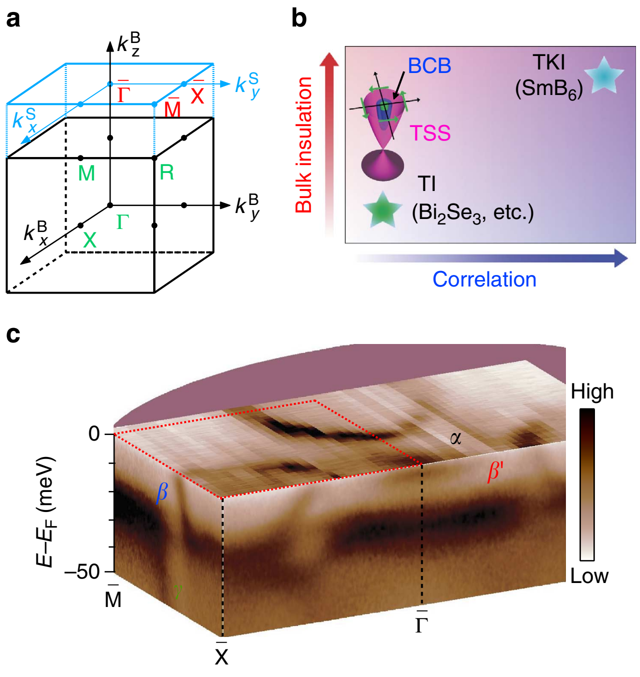

Figure 1 | Electronic structure of SmB_6 and its comparison with non-interacting TIs. (**a**) The first Brillouin zone of SmB_6 and the projection on the cleaved surface. High-symmetry points are also indicated. (**b**) Illustration showing the electronic correlation and bulk insulating nature of Bi_2Se_3 and the TKI SmB_6. The inset shows the electronic structure and spin texture of Bi_2Se_3. (**c**) 3D intensity plot of the photoemission data, showing the FS and electronic structure of SmB_6 measured with a photon energy of 26 eV and energy resolution <5 meV at $T = 1$ K. We define the surface bands at the $\bar{\Gamma}$ and $\bar{X}$ points as α and β, and the bulk valence d-band as γ, which are consistent with a previous study[7].

Results

Spin polarization of the TSS along the $\bar{X}$-$\bar{\Gamma}$-$\bar{X}$ direction. In Fig. 2b, we plot the near-E_F spin-integrated ARPES intensity and a momentum distribution curve (MDC) at E_{SR} (10 meV above E_F) along the $\bar{X}$-$\bar{\Gamma}$-$\bar{X}$ direction. The momentum cut in the SBZ is indicated by the red line (C1) in the FS mapping (Fig. 2a). The spin-integrated ARPES data shown in Fig. 2a,b are taken with $h\nu = 26$ eV ($k_z = 4\pi$ for the bulk states) at the same experimental station as the SARPES data discussed in the following. The sample temperature for the spin-integrated and SARPES measurements is 20 K, at which the Kondo gap is fully opened and the surface states dominate near E_F[7,15–19]. Inside the Kondo band gap, the α- and β-surface state bands are visible in the intensity plot, which are also clearly seen as peaks of the MDC at E_{SR}. Photon energy-dependent measurements have shown that these bands do not disperse in k_z, the momentum along the surface normal, and thus are true surface states[7,16–18]. To determine the spin polarization of the surface bands, we performed spin-resolved MDC measurements along the $\bar{X}$-$\bar{\Gamma}$-$\bar{X}$ cut (C1) at E_{SR}. The purpose of choosing the MDC to lie at E_{SR} is to minimize the contribution of the bulk f and d states located at $E_B \geq 20$ meV due to the limited energy resolution in spin-resolved mode (see Methods). At the same time, the count rate still allows us to acquire data with sufficient statistics in the SARPES measurements. Figure 2c,e,g shows the spin-resolved MDC intensity $I^{\uparrow\downarrow}{}_{x,y,z}$ in the x, y and z directions, respectively, measured with $h\nu = 26$ eV and right-hand circularly polarized light (C+). The in-plane spin polarization x and y axes are defined along each $\bar{\Gamma}$-$\bar{X}$ direction (x and y as indicated in the coordinate system in Fig. 2a), and the out-of-plane spin polarization z axis is along the sample normal k_z. As shown in Fig. 2c,d, there is a clear difference in $I^{\uparrow}{}_x$ and $I^{\downarrow}{}_x$ at each of the two MDC main peaks that correspond to two branches of the β-bands, indicating that the surface state bands are spin-polarized along the x direction. We have also observed two more peaks between the main β-band peaks in the spin-polarization spectrum along the x direction (Fig. 2d). These are ascribed to the β'-band (Fig. 1c), which results from the folding of β due to a surface reconstruction assuming a single domain[7,17]. We notice that the β'-band is hardly resolved from the β-band in the spin-integrated spectra (Fig. 2b) due to the limited resolution. However, it can be observed clearly in the spin-resolved spectra because of the different spin polarization. Combining the SARPES data in Fig. 2, we can summarize that near E_F the β- and β'-bands measured along C1 are both polarized in the x direction, as indicated by the coordinate system in Fig. 2a. Moreover, each of the pairs of

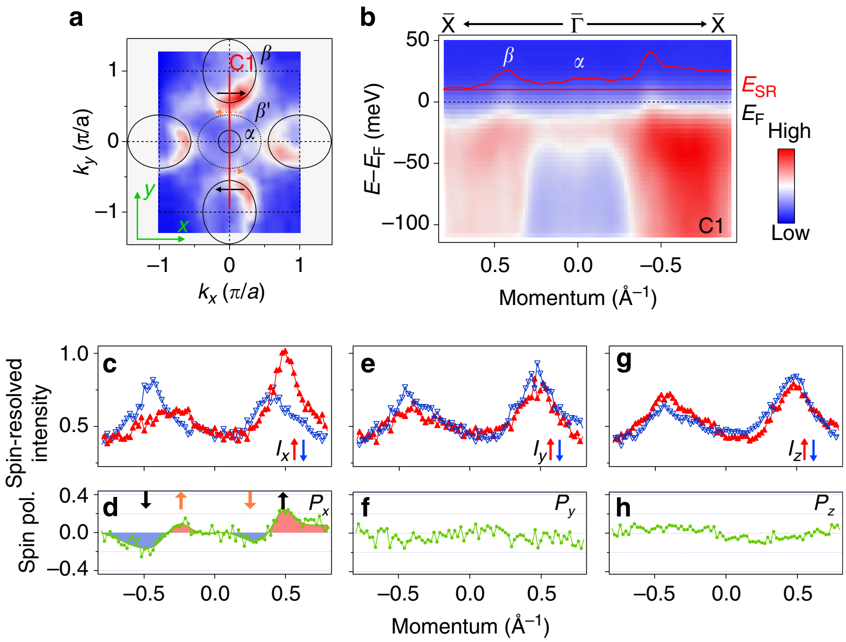

Figure 2 | Spin polarization of topological Dirac surface states along the $\bar{X}$-$\bar{\Gamma}$-$\bar{X}$ direction. (**a**) FS map of SmB_6. (**b**) Low energy excitations near E_F along the high-symmetry line $\bar{X}$-$\bar{\Gamma}$-$\bar{X}$. The location in the k_x-k_y plane is indicated by C1 in **a**. The red curve is the MDC at E_{SR} (10 meV above E_F). (**c**) Measured spin-resolved intensity projected on the *x* direction for the surface states at E_{SR}. The red and blue symbols are the intensity of spin-up and spin-down states, respectively. (**d**) Spin polarization along the *x* direction for the surface states measured at the E_{SR}. The red and blue colour regions represent positive and negative spin polarizations (spin-up and spin-down), respectively. The black and orange arrows represent the spin polarization directions of the β- and β'-bands along the *x* axis, respectively. (**e**,**f**) Same as **c**,**d** but along the *y* direction. (**g**,**h**) Same as **c**,**d** but along the *z* (out-of-plane) direction. All the results in Fig. 2 are measured with a photon energy of 26 eV and right-hand circular polarization (C +).

β- and β'-states located at **k** and -**k** have opposite spin polarizations, consistent with the behaviour of a spin-split Kramers pair, in accordance with TRS.

Spin polarization of the TSS along high symmetry lines. To determine the spin texture of the FS pockets, we have carried out SARPES measurements along the cuts C1–C4, as indicated in Fig. 3a, using C + polarized light and photon energies of $h\nu = 26$ and 30 eV. For both photon energies, a consistent spin texture was obtained. As shown in Fig. 3c, the spin polarization (MDC at E_{SR}) measured with $h\nu = 30$ eV along C1 is essentially the same as that in Fig. 2d taken with $h\nu = 26$ eV. Figure 3d shows the spin polarization along C2 (perpendicular to C1). Similar to the observation along C1, the β- and β'-bands are spin polarized, but now along the *y* direction. At the two $\mathbf{k}_F$ points on cut C3 (C4), the spin polarizations of the β-band are opposite along the *x* (*y*) direction (Fig. 3e,f). The determined spin texture is summarized in Fig. 3a with spin polarizations marked by arrows. The measured spin texture, wherein the spin polarization is locked to the momentum, is fully consistent with TSS in the sense that it obeys both TRS and the crystal symmetry. This is further supported by the fact that the folded band β' has the same spin texture as the original band β, as expected from a simple Umklapp mechanism[22].

Photon polarization-dependent SARPES results. It has been shown that a spin polarization signal can also appear in the photoemission process from states that possess no net spin polarization[23]. This so-called photoemission effect is discussed, for instance, for the core-level photoelectrons from non-magnetic solids[24], the bulk valence bands of TIs[25], as well as the bulk *f* states of SmB_6 (ref. 26). In contrast to the intrinsic spin signal from the spin-polarized initial states, the non-intrinsic spin signal caused by the photoemission effect depends on the incident photon energy and polarization. For example, the non-intrinsic spin polarization of the *f* states in SmB_6 caused by the photoemission effect changes direction when the photon polarization changes from C + to left-hand circularly polarized light (C-), and vanishes with linear polarization (l-pol)[26]. The consistent momentum-locked spin texture obtained with different photon energies (Figs 2 and 3) in our experiments provides evidence that the observed spin polarizations are intrinsic to the spin-polarized initial states. To rule out the possibility that the detected spin texture results from the polarization of the incident light, we conducted spin-resolved measurements using incident light with all available polarizations. Figure 3f,g,i shows the results along C4 detected by using C +, C − and linear polarizations of the incident light. The same spin polarizations from differently polarized light give further confidence that the observed spin polarizations reflect the intrinsic spin structure of the initial states.

No spin polarization of the bulk states. As any spin polarization of the bulk *f* states caused by a photoemission effect should be vanish with linearly polarized light[26], the results obtained with the linearly polarized light (Fig. 3h,i) further indicate that the spin polarization originates from the surface β-band, and not from contamination of the bulk *f* states due to the limited energy resolution used in SAPRES measurements. To further exclude contamination from the bulk *d* states as an origin of the observed spin polarizations of the MDCs studied at E_{SR}, we performed measurements at a higher binding energy (E_{HB} as illustrated in Fig. 3b), where the bulk *d* states dominate the photoemission intensity. Figure 3j,k shows the spin-resolved MDC intensity $I^{\uparrow\downarrow}$ and the spin polarization spectra along the *y* direction, taken with

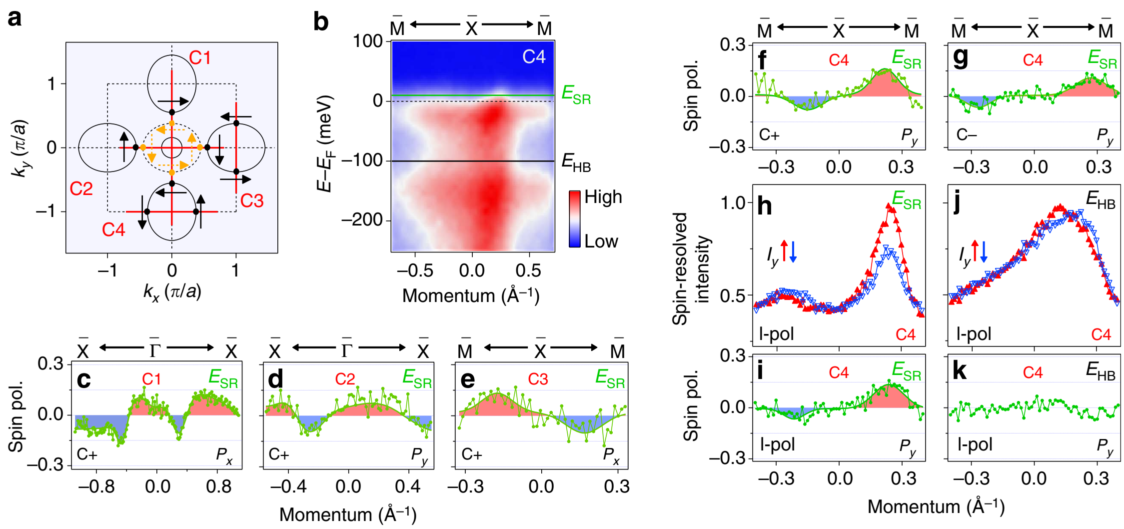

Figure 3 | Spin polarization of topological Dirac surface states along high-symmetry lines. (**a**) Schematic showing the FS of the topological surface states in SmB_6, with red lines indicating the locations of spin measurements in the k_x–k_y plane, labelled as C1, C2, C3 and C4. The circle at the BZ centre $\bar{\Gamma}$ point and ellipses at the middle points of BZ boundaries ($\bar{X}$ points) indicate the FSs of the α- and β-bands, respectively[7,17]. The dashed line ellipse at the $\bar{\Gamma}$ point indicates the folded band β'[7,17]. The dots are the k_F positions of the bands and the arrows are the measured spin polarizations at the positions of the dots. The black dashed lines indicate the first SBZ. (**b**) Low-energy excitations near E_F along the high symmetry line $\bar{M}$-$\bar{X}$-$\bar{M}$, measured with photon energy $h\nu = 30$ eV and C + polarization. The location in the k_x–k_y plane is indicated by C4 in **a**. (**c**) Spin polarization measured at $h\nu = 30$ eV along the x direction for the surface states at E_{SR} (10 meV above E_F). The location in the k_x–k_y plane is indicated by C1 in **a**. (**d**) Analogous to **c**, but for C2, where the spin polarization direction is along y. (**e**) Analogous to **c**, but measured at $h\nu = 26$ eV for C3, where the spin polarization direction is along x. (**f**) Analogous to **c**, but for C4, where the spin polarization direction is along y. For (**c**–**f**), the photon polarization is C +. (**g**) Same as **f**, but with C− photon polarization. (**h**) Measured spin-resolved intensity along the y direction for the surface states at E_{SR}, measured at $h\nu = 30$ eV with linear light polarization. The red and blue symbols are the intensity of spin-up and spin-down states, respectively. The location in the k_x–k_y plane is indicated by C4 in **a**. (**i**) Spin polarization along the y direction for the surface states at the E_{SR}. (**j**,**k**) Same as **h**,**i** but for the bulk states at higher binding energy illustrated by E_{HB} in **b**.

linearly polarized light (l-pol). In contrast to the spectra at E_{SR} (Fig. 3h,i), the spin-resolved MDCs at E_{HB} show negligible difference, indicating that the photoelectrons from the spin-degenerate bulk d-states are not spin polarized. Therefore, we conclude that the spin signal at E_{SR} is dominated by the surface states, which provides compelling evidence that SmB_6 is the first realization of a TKI.

Discussion

Figure 4 schematically summarizes our main experimental finding of the spin structure of the surface bands of SmB_6. For simplicity, we consider the situation without folding bands. The spin orientations of the electrons in the in-gap surface β-band, which is located between the strongly localized bulk f states and the chemical potential, are locked to their momenta; namely, at opposite momenta (**k** and -**k**), the surface states have opposite spins. This anti-clockwise spin texture for the surface band in SmB_6 shows a great similarity to other 3D TIs (Bi_2Se_3, Bi_2Te_3, etc.), which each has a FS from a single pocket centred at the $\bar{\Gamma}$point in the SBZ[27,28]. Extensive ARPES studies have shown that SmB_6 has a surface FS formed by three electron pockets with Kramers points located around the SBZ centre and boundary[7,16,17]. The revealed spin texture, together with the odd number of pockets, is consistent with the metallic states at the surface of SmB_6 being non-trivial topological surface states, and the findings here strongly support recent theoretical predictions that SmB_6 is a TKI[4–6]. A crucial and so far unresolved problem for the real-world implementation of TIs is that most 3D TI candidates are not bulk-insulating[4,29]. On the other hand, SmB_6 is a mixed valence Kondo insulator. Owing to the hybridization of the nearly localized $4f$ bands with the

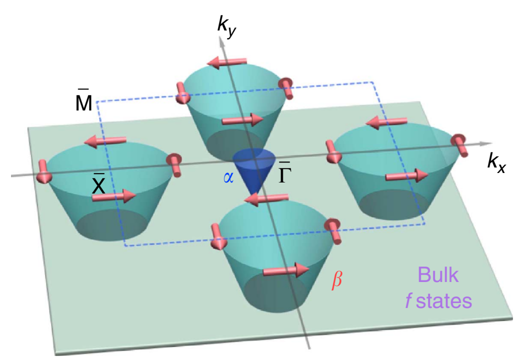

Figure 4 | Schematic of the spin-polarized surface state dispersion in the TKI SmB_6. The blue and green curved surfaces centred at the $\bar{\Gamma}$ and $\bar{X}$ points represent the α- and β-bands, respectively. The plane sitting below represents the bulk f states. The spin polarizations of the β-band are indicated with red arrows. The shape and size of the α-band are from refs 7,17. The blue dashed lines indicate the first SBZ.

dispersive conduction band, a band gap opens near the chemical potential at low temperature, leading the system in to a good bulk insulator[4,30–32]. Thus, the direct identification of SmB_6 as a TKI is a significant advance in realizing a topological quantum state of matter in which the metallic edge states, protected by TRS, are located on a true bulk insulator. It is also worthwhile to mention that the metallic TSS formed by the electron pockets at low temperatures can provide a natural explanation for the longstanding puzzle that the resistivity in SmB_6 saturates to a finite value instead of being divergent[30–32]. Meanwhile, the coexistence of the topological surface states and the strongly correlated bulk states offers new opportunities for understanding TIs beyond the non-interacting topological theory.

Methods

(S)ARPES measurements. SARPES and ARPES measurements were performed at the Surface/Interface Spectroscopy beamline at the Swiss Light Source with the COPHEE station. The two orthogonally mounted 40 kV classical Mott detectors allow for the determination of all three components of the spin of the electron (P_x, P_y and P_z) as a function of its energy and momentum[33,34]. To achieve this, the spin polarization curves obtained for the three spatial directions are fitted simultaneously with the sum of all the Mott channels, that is, the spin integrated signal. Further technical details of the data acquisition and analysis can be found in ref. 35. The SARPES measurements were repeated for several samples with photon energies ranging from 26 to 30 eV and with circular and linear light polarizations. Results with different photon energies and light polarizations are consistent. All the spin-integrated and spin-resolved data shown in Figs 2 and 3 are taken at $T = 20$ K, where the Kondo gap is fully open[7,15–18]. The energy and angle resolutions were 60 meV (full width at half maximum) and 3% of the SBZ, respectively, to allow for acceptable statistics. Because of the low photoemission signal, the typical duration of a spin-resolved MDC was about 6 h. After this period, the sample quality was confirmed again by spin-integrated measurements. Clean surfaces for the (S)ARPES measurements were obtained by cleaving the crystals *in situ* at low temperature (20 K) in a working vacuum better than 2×10^{-10} mbar. Shiny mirror-like surfaces were obtained after cleaving the samples, confirming their high quality.

Sample fabrication. High-quality single crystals of SmB_6 were obtained by growth from Al-flux using samarium pieces (99.9%), boron powder (99.99%) and aluminum pieces in a ratio of 0.5 g of Sm:B (1:6) and 50 g of Al (99.99%). The growth was done in a vertical gradient furnace under continues argon flow at a temperature up to 1,500 °C with a cooling rate of $5\,K\,h^{-1}$. The aluminum flux was removed by potassium hydroxide solution. The crystals, which are millimetre sized, have a bar shape, black colour and flat, mirror-like surfaces.

References

1. Ando, Y. Topological insulator materials. *J. Phys. Soc. Jpn* **82,** 102001 (2013).
2. Hasan, M. Z. & Kane, C. L. Colloquium: topological insulators. *Rev. Mod. Phys.* **82,** 3045–3067 (2010).
3. Qi, X.-L. & Zhang, S.-C. Topological insulators and superconductors. *Rev. Mod. Phys.* **83,** 1057–1110 (2011).
4. Dzero, M., Sun, K., Galitski, V. & Coleman, P. Topological Kondo insulators. *Phys. Rev. Lett.* **104,** 106408 (2010).
5. Dzero, M., Sun, K., Coleman, P. & Galitski, V. Theory of topological Kondo insulators. *Phys. Rev. B* **85,** 045130 (2012).
6. Lu, F., Zhao, J.-Z., Weng, H.-M., Fang, Z. & Dai, X. Correlated topological insulators with mixed valence. *Phys. Rev. Lett.* **110,** 096401 (2013).
7. Xu, N. *et al.* Surface and bulk electronic structure of the strongly correlated system SmB_6 and implications for a topological Kondo insulator. *Phys. Rev. B* **88,** 121102(R) (2013).
8. Wolgast, S. *et al.* Low temperature surface conduction in the Kondo insulator SmB_6. *Phys. Rev. B* **88,** 180405(R) (2013).
9. Kim, D. J. *et al.* Surface hall effect and nonlocal transport in SmB_6: evidence for surface conduction. *Sci. Rep.* **3,** 3150 (2013).
10. Thomas *et al.* Weak antilocalization and linear magnetoresistance in the surface state of SmB_6. Preprint at http://arxiv.org/abs/1307.4133 (2013).
11. Li, G. *et al.* Quantum oscillations in Kondo insulator SmB_6. Preprint at http://arxiv.org/abs/1306.5221 (2013).
12. Kim, D. J., Xia, J. & Fisk, Z. Topological surface state in the Kondo insulator samarium hexaboride. *Nat. Mater.* **13,** 466 (2014).
13. Chen, F. *et al.*Angular dependent magnetoresistance evidence for robust surface state in Kondo insulator SmB_6. Preprint at http://arxiv.org/abs/1309.2378 (2013).
14. Yue, Z.-J., Wang, X.-L., Wang, D.-L., Dou, S.-X. & Wang, J.-Y. Four-fold symmetric magnetoresistance in Kondo insulator SmB_6. Preprint at http://arxiv.org/abs/1309.3005 (2013).
15. Zhang, X.-H. *et al.* Hybridization, inter-ion correlation, and surface states in the Kondo insulator SmB_6. *Phys. Rev. X* **3,** 011011 (2013).
16. Neupane, M. *et al.* Surface electronic structure of a topological Kondo insulator candidate SmB_6: insights from high-resolution ARPES. *Nat. Commun.* **4,** 2991 (2013).
17. Jiang, J. *et al.* Observation of in-gap surface states in the Kondo insulator SmB_6 by photoemission. *Nat. Commun.* **4,** 3010 (2013).
18. Denlinger, J. D. *et al.*Temperature dependence of linked gap and surface state evolution in the mixed valent topological insulator SmB_6. Preprint at http://arxiv.org/abs/1312.6637 (2013).
19. Yee, M. M. *et al.*Imaging the Kondo insulating gap on SmB_6. Preprint at http://arxiv.org/abs/1308.1085 (2013).
20. Zhu, Z.-H. *et al.* Polarity-driven surface metallicity in SmB_6. *Phys. Rev. Lett.* **111,** 216402 (2013).
21. Frantzeskakis, E. *et al.* Kondo hybridisation and the origin of metallic states at the (001) surface of SmB_6. *Phys. Rev. X* **3,** 041023 (2013).
22. Lobo-Checa, J. *et al.* Robust spin polarization and spin textures on stepped Au(111) surfaces. *Phys. Rev. Lett.* **104,** 187602 (2010).
23. Heinzmann, U. & Dil, J. H. Spin–orbit-induced photoelectron spin polarization in angle-resolved photoemission from both atomic and condensed matter targets. *J. Phys. Condens. Matter* **24,** 173001 (2012).
24. Starke, K. *et al.* Spin-polarized photoelectrons excited by circularly polarized radiation from a nonmagnetic solid. *Phys. Rev. B* **53,** R10544(R) (1996).
25. Jozwiak, C. *et al.* Widespread spin polarization effects in photoemission from topological insulators. *Phys. Rev. B* **84,** 165113 (2011).
26. Suga, S. *et al.* Spin-polarized angle-resolved photoelectron spectroscopy of the so-predicted Kondo topological insulator SmB_6. *J. Phys. Soc. Jpn* **83,** 014705 (2014).
27. Hsieh, D. *et al.* A tunable topological insulator in the spin helical Dirac transport regime. *Nature* **460,** 1101–1105 (2009).
28. Eremeev, S. V. *et al.* Atom-specific spin mapping and buried topological states in a homologous series of topological insulators. *Nat. Commun.* **3,** 635 (2012).
29. Muff, S. *et al.* Separating the bulk and surface n- to p-type transition in the topological insulator $GeBi_{4-x}Sb_xTe_7$. *Phys. Rev. B* **88,** 035407 (2013).
30. Menth, A., Buehler, E. & Geballe, T. H. Magnetic and Semiconducting Properties of SmB_6. *Phys. Rev. Lett.* **22,** 295–297 (1969).
31. Allen, J. W., Batlogg, B. & Wachter, P. Large low-temperature Hall effect and resistivity in mixed-valent SmB_6. *Phys. Rev. B* **20,** 4807–4813 (1979).
32. Cooley, J. C., Aronson, M. C., Fisk, Z. & Canfield, P. C. SmB_6: Kondo insulator or exotic metal? *Phys. Rev. Lett.* **74,** 1629–1632 (1995).
33. Hoesch, M. *et al.* Spin-polarized Fermi surface mapping. *J. Electron Spectrosc. Relat. Phenom.* **124,** 263 (2002).
34. Dil, J. H. Spin and angle resolved photoemission on non-magnetic low dimensional systems. *J. Phys. Condens. Matter* **21,** 403001 (2009).
35. Meier, F., Dil, J. H. & Osterwalder, J. Measuring spin polarization vectors in angle-resolved photoemission spectroscopy. *New J. Phys.* **11,** 125008 (2009).

Acknowledgements

This work was supported by the Sino-Swiss Science and Technology Cooperation (project number IZLCZ2138954), the Swiss National Science Foundation (grant number 200021-137783 and PP00P2_144742) and MOST (grant number 2010CB923000) and NSFC.

Author contributions

N.X., J.H.D. and M.S. conceived the experiments. N.X., J.H.D., R.S.D., G.L., S.M. and X.S. carried out the experiments with assistance from C.E.M., N.C.P., M.R. and S.V.B.; N.X., J.H.D. and M.S. analysed the data with valuable feedback from R.Y., H.M.W., Z.F., X.D., J.M. and H.D.; P.K.B., E.P., K.C. and A.A. synthesized the samples; N.X., J.H.D. and M.S. wrote the manuscript. All authors discussed the results and commented on the manuscript.

Additional information

Competing financial interests: The authors declare no competing financial interests.

Reprints and permission information is available online at http://npg.nature.com/reprintsandpermissions/

How to cite this article: Xu, N. *et al.* Direct observation of the spin texture in SmB_6 as evidence of the topological Kondo insulator. *Nat. Commun.* 5:4566 doi: 10.1038/ncomms5566 (2014).